# Anomalous inverse spin Hall effect in perpendicularly magnetized Co/Pd multilayers

Man Yang [1,*] Bingfeng Miao,[1,*,†] Jun Cheng,[1] Kang He,[1] Xi Yang,[1] Yulun Zeng,[1] Ziqiang Wang,[1] Liang Sun,[1] Xiangrong Wang,[2,3,‡] Antonio Azevedo,[4] Subhankar Bedanta,[5] and Haifeng Ding[1,§]

[1] *National Laboratory of Solid State Microstructures, Department of Physics, Nanjing University and Collaborative Innovation Center of Advanced Microstructures, Nanjing 210093, People's Republic of China*

[2] *Physics Department, The Hongkong University of Science and Technology, Clear Water Bay, Kowloon, Hongkong*

[3] *PHKUST Shenzhen Research Institute, Shenzhen 518057, People's Republic of China*

[4] *Departamento de Física, Universidade Federal de Pernambuco, Recife, Pernambuco 50670-901, Brasil*

[5] *Laboratory for Nanomagnetism and Magnetic Materials (LNMM), School of Physical Sciences, National Institute of Science Education and Research (NISER), An OCC of Homi Bhabha National Institute (HBNI), Jatni-752050, India*

(Received 4 April 2022; revised 3 June 2022; accepted 21 June 2022; published 29 June 2022)

The spin Hall effect (SHE) and the inverse spin Hall effect (ISHE) have been widely utilized to interconvert the charge and spin currents. In them, the charge current, spin current, and spin polarization are orthogonal to each other, limiting their applications. Based on the general tensor requirement of the spin-charge conversion, additional possibilities can be introduced when the order parameter, the magnetization of a ferromagnet, is involved. We herein report the spin-charge conversion in perpendicular magnetized Co/Pd multilayers with spin pumping measurements. We unambiguously observed the anomalous inverse spin Hall effect (AISHE), where the charge current is collinear with the spin polarization. Both the sign and magnitude of AISHE can be linearly regulated by the out-of-plane magnetization of Co/Pd multilayers. Further, the observed amplitude ratio of AISHE/ISHE in spin pumping measurements is independent of the applied microwave frequency, indicating that it is a material specific parameter.

DOI: 10.1103/PhysRevB.105.224426

Spin current is a central component of modern spintronics. It can carry information in a spintronic circuitry and perform different kinds of functionalities, like what its electric current counterpart does in electronics, but consumes much less energy [1,2]. Spin current has been widely used for switching magnetization [3–5], driving domain walls [6], and skyrmions motion [7] via spin-orbit torque. Thus, it has strong potential in various applications such as magnetic storage [8,9], field sensors [10], and logic devices [11], etc. Unlike electric current, which is the flow of an electric charge scalar, a spin current is the flow of an angular momentum vector. Therefore, a spin current is a rank-2 tensor with nine components in three dimensions.

The conventional spin Hall effect (SHE) [Fig. 1(a)] and its reciprocal effect, the inverse SHE (ISHE) [Fig. 1(b)] enable the interconversion between spin current and charge current. In the Cartesian coordinates, a charge current $J_k^c$ along the direction $\hat{k}$ can generates a spin current $J_{ij}^s$, which is polarized along the direction $\hat{j}$ and flowing along the direction $\hat{i}$, i.e., $J_{ij}^s = \theta_0 \frac{\hbar}{2e}\varepsilon_{ijk}J_k^c$. Here, $i$, $j$, $k = 1, 2, 3$ stand for the directions along $x$, $y$, and $z$ axes, $\varepsilon_{ijk}$ is the Levi-Civita symbol, and the Einstein summation convention is applied. $\theta_0$ is a dimensionless material parameter called the spin Hall angle, which determines the efficiency of interconversion between spin and charge currents. ISHE converts $J_{ij}^s$ into $J_k^c$ as $J_k^c = \frac{2e}{\hbar}\theta_0'\varepsilon_{ijk}J_{ij}^s$. $\theta_0'$ is called inverse spin Hall angle, and $\theta_0' = \theta_0$ due to the Onsager reciprocity. The mutual orthogonalization of charge current, spin current, and spin polarization strongly limits the applications of the SHE and ISHE. For instance, the most efficient magnetic switching based on the change in the effective damping of the magnetic layer is only realized for the in-plane magnetized materials [4,12,13]. For the deterministic switching of perpendicular magnetization, which is desired for maximizing device density, an effective symmetry-breaking field with a component along the current direction is typically required [3,14–17].

Magnetic materials with the order parameter magnetization **M** for the ferromagnet may overcome the limitation of the conventional SHE and ISHE [18]. In general, the spin Hall angle $\theta_{ijk}^{\mathrm{SH}}$ is a tensor of rank 3 in the charge-spin conversion and is defined with $J_{ij}^s = \frac{\hbar}{2e}\theta_{ijk}^{\mathrm{SH}}J_k^c$. Based on the general tensor requirement of a physical quantity, it can be written as [18]

$$\begin{aligned}\theta_{ijk}^{\mathrm{SH}} &= \theta_0\varepsilon_{ijk} + \theta_1 M_l\varepsilon_{iln}\varepsilon_{jnk} + \theta_2 M_l\varepsilon_{ink}\varepsilon_{jln}\\ &= \theta_0\varepsilon_{ijk} + [(\theta_1+\theta_2)\delta_{ij}\delta_{kl\neq i} + \theta_1\delta_{ik}\delta_{jl\neq i} + \theta_2\delta_{il}\delta_{jk\neq l}]M_l,\end{aligned} \tag{1}$$

where $\theta_1$ and $\theta_2$ are two anomalous SHE (ASHE) coefficients when the magnetization and the charge current are perpendicular, and the spin current is along/perpendicular to the charge current direction, respectively. This means that a

*These authors contributed equally to this work.
†Corresponding author: bfmiao@nju.edu.cn
‡Corresponding author: phxwan@ust.hk
§Corresponding author: hfding@nju.edu.cn

 

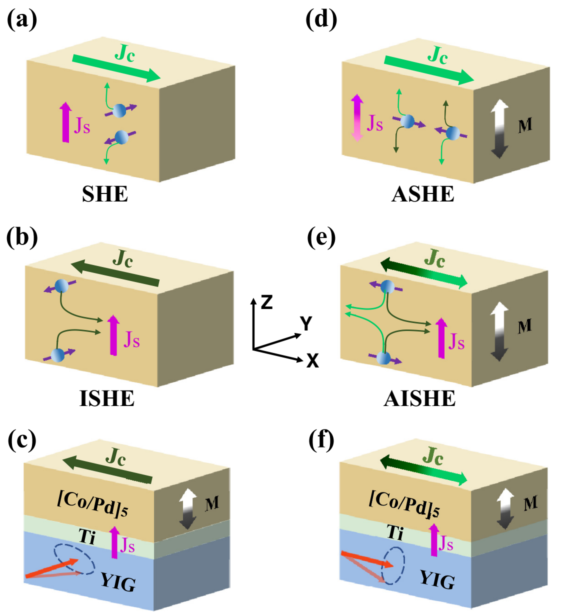


FIG. 1. Schematic illustrations of (a) the spin Hall effect (SHE), (b) inverse spin Hall effect (ISHE). (c) Sketch of the measurement geometry for the ISHE. Panels (d) and (e) are the schematic illustrations of the anomalous spin Hall effect and anomalous inverse spin Hall effect, respectively. (f) Sketch of the measurement geometry for the anomalous ISHE (AISHE). The spin current is generated by the precession of the magnetization of YIG ($Y_3Fe_5O_{12}$) and the AISHE is conducted in perpendicularly magnetized $[Co/Pd]_5$ multilayers.

charge current perpendicular to the magnetization can generate orthogonal spin current whose propagation direction and polarization are not only orthogonal to each other but also along either the charge current or the magnetization direction [Fig. 1(d) describes the latter case]. Conversely, external spin current $J^s_{ij}$ passing through a ferromagnet can generate a charge current $J^c_k$, via $J^c_k = \frac{2e}{\hbar}\theta^{\mathrm{ISH}}_{ijk}J^s_{ij}$, where $\theta^{\mathrm{ISH}}_{ijk}$ is the inverse spin Hall angle tensor of rank 3. The general $\theta^{\mathrm{ISH}}_{ijk}$ in the ferromagnet can be described as [18]

$$\theta^{\mathrm{ISH}}_{ijk} = \theta'_0\varepsilon_{ijk} + [(\theta'_1 + \theta'_2)\delta_{ij}\delta_{kl\neq i} + \theta'_1\delta_{ik}\delta_{jl\neq i} + \theta'_2\delta_{il}\delta_{jk\neq l}]M_l, \tag{2}$$

where $\theta'_1$ and $\theta'_2$ are coefficients that characterize the anomalous ISHE (AISHE). The AISHE can therefore convert an orthogonal spin current into a charge current along either the spin propagation direction or the polarization direction [Fig. 1(e)]. Equally important, the converted spin or charge current reverses its direction when **M** of the ferromagnet flips. We note that the spin current in antiferromagnets [19–21] and materials with low crystalline symmetry [13,22,23] may also enrich the scope of the conventional SHE and ISHE. However, compared to the Néel order of antiferromagnets and the crystalline symmetry, **M** of the ferromagnet can be readily controlled, thus providing a versatile and convenient method to modulate the property of the generated anomalous spin current.

The ASHE and AISHE with charge current collinear with spin polarization [Figs. 1(d) and 1(e)] can possibly be explained by several mechanisms such as the spin swapping effect [24], interface spin-orbit precession effect [25,26], spin precession motion in diffusive ferromagnets [27], etc. And the spin torque from ASHE schematized in Fig. 1(d) has been demonstrated by Humphries *et al.* via magneto-optic-Kerr effect [28], and by Wang *et al.* and Hibino *et al.* via spin-torque ferromagnetic resonance and harmonic Hall measurements [29–33]. Very recently, Chuang *et al.* and Yagmur *et al.* reported the magnetization dependent spin charge conversion in Pt/Co/Pt/YIG [34] and $Tb_xCo_{100-x}/Pt/YIG$ [35] with thermally injected spin current via the spin Seebeck effect in yttrium iron garnet (YIG). It is worthwhile to mention that there is an effect with a similar name, the spin anomalous Hall effect [36], albeit it has another physical origin when compared to the ASHE discussed here.

In this work, we investigate the spin-charge conversion of the perpendicularly magnetized Co/Pd multilayers, where in-plane magnetized YIG film acts as the source of the spin current. We use spin pumping, which is the most versatile technique to study the frequency dependence of the spin-charge conversion phenomena [37–39] and has been used to study the AISHE in Co/Ni multilayers very recently [33]. YIG is a ferrimagnetic insulator with low damping which can be epitaxially grown on GGG ($Gd_3Ga_5O_{12}$) substrate [40]. Due to its high resistivity, YIG has been widely used as a main spin current source with little influence on electrical measurements. In addition, Co/Pd multilayers can have strong perpendicular magnetic anisotropy (PMA) due to the accumulation of the interface anisotropy [41], where Pd has relatively weak spin orbit coupling [42]. Our results show that the AISHE is a general feature of a ferromagnet, independent of the experimental approach. We also found that a direct linear relation between the AISHE signal and the Co/Pd magnetization can be established. Furthermore, we observed a frequency-independent ratio of AISHE/ISHE signal of Co/Pd multilayers, indicating that it is a material specific parameter.

At the ferromagnetic resonance (FMR) condition of the YIG film, the magnetization precesses and pumps a dc spin current into its adjacent metallic multilayer, with the spin polarization aligned along the equilibrium direction of the magnetization of the YIG film [37,38]. Experimentally, the voltage lead along the $x$ direction only detects the charge current converted from ISHE when the external magnetic field is applied along the $y$ direction [Fig. 1(c)]. Since ISHE is independent of the magnetization orientation, the measured signal is expected to be irrelevant with the magnetization orientation of the metallic ferromagnetic layer [43,44]. On the other hand, AISHE of Co/Pd multilayers emerges when the YIG magnetization precesses around the $x$ direction [Fig. 1(f)]. As discussed above, AISHE has three distinct features in comparison to ISHE. First, it changes sign when the magnetization reverses its orientation while ISHE is independent of the magnetization orientation. Second, ISHE requires $\mathbf{J_C}\perp\mathbf{J_S}\perp\boldsymbol{\sigma}$ but $\boldsymbol{\sigma}$ is no longer required to be perpendicular to both $\mathbf{J_S}$ and $\mathbf{J_C}$ for the AISHE. In the specific geometry discussed in Fig. 1(f); it is collinear with $\mathbf{J_C}$. Further, its amplitude is linearly proportional to **M**.

The sample used to investigate the spin transport properties is the YIG(114 nm)/Ti(3 nm)/Co (0.6 nm)/Pd(2 nm)/[Co(0.4 nm)/Pd(2 nm)]$_4$ multilayer, simplified as YIG/Ti/$[Co/Pd]_5$. The 114-nm YIG single

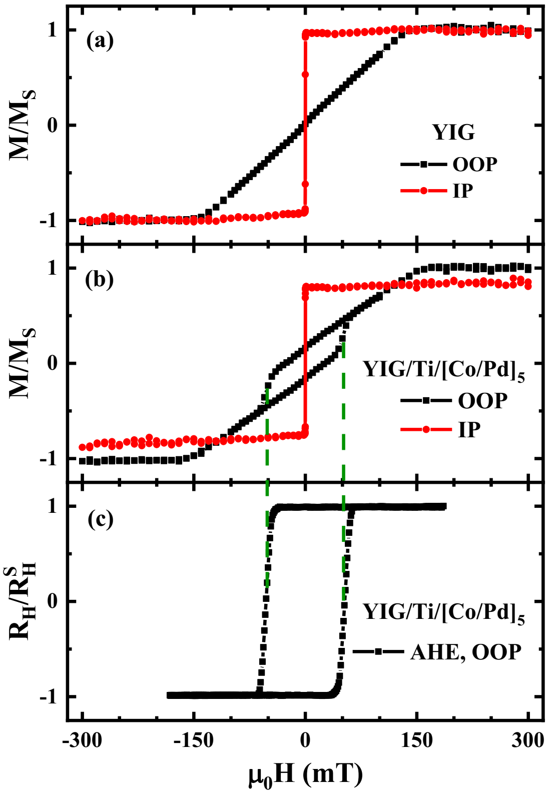


FIG. 2. The normalized in-plane (IP, red curves) and out-of-plane (OOP, black curves) hysteresis loops of (a) YIG film, (b) YIG/Ti/[Co/Pd]$_5$. YIG film and [Co/Pd]$_5$ multilayers exhibit a well-defined in-plane and out-of-plane anisotropy, respectively. (c) Anomalous Hall effect measurement of YIG/Ti/[Co/Pd]$_5$ with magnetic field sweeping perpendicular to the multilayer. Note: the switching fields correspond to the fields for the abrupt jump of magnetization observed in OOP loop of YIG/Ti/[Co/Pd]$_5$ shown in (b).

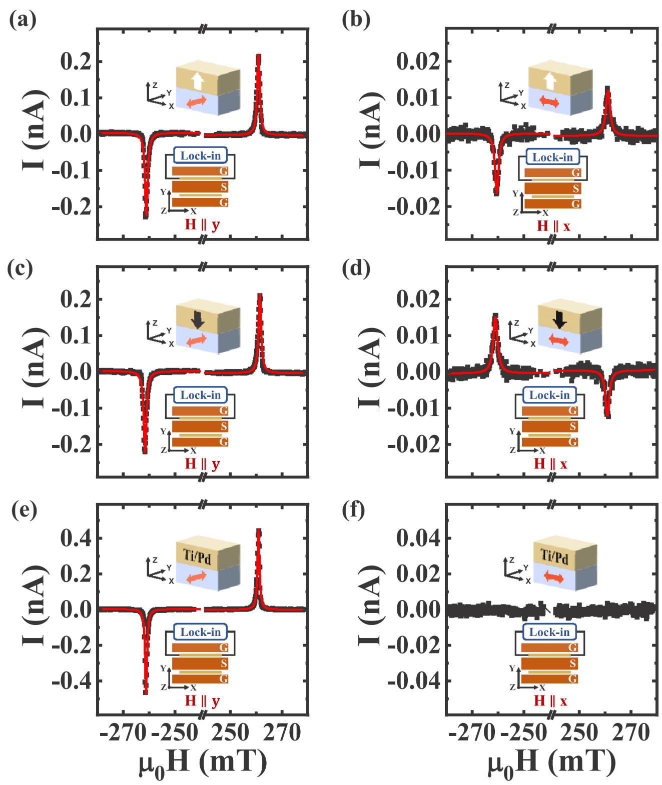


FIG. 3. (a)–(d) are measurements of spin pumping current of Ti/[Co/Pd]$_5$ at 9 GHz. Panels (a) and (b) are when the magnetization of Ti/[Co/Pd]$_5$ is along the $+z$ direction and the magnetic field is applied along the $y$ direction and $x$ direction, respectively. Panels (c) and (d) are similar measurements, however, the magnetization of Ti/[Co/Pd]$_5$ is along the $-z$ direction. Panels (e) and (f) are the measurements of the spin pumping currents of Ti/Pd at 9 GHz when the magnetic field is applied along the $y$ direction and $x$ direction, respectively.

crystalline film is prepared by the radio frequency (rf) magnetron sputtering on GGG(111) substrate at room temperature with postannealing at 800 °C for 1 h at the ambient atmosphere. Metallic Ti/[Co/Pd]$_5$ multilayers are prepared by dc magnetron sputtering at room temperature, where Co/Pd multilayers have strong PMA. Here, the light metal Ti serves as a buffer layer that decouples the magnetization of Co/Pd multilayers from the magnetization of the YIG film. For the spin pumping measurements, we patterned the Co/Pd multilayers into strips with photolithography and further fabricated a coplanar waveguide (CPW) with a characteristic impedance of 50 Ω from 100-nm-thick Cu directly deposited on top of the YIG film with dc magnetron sputtering. The Co/Pd multilayer strips are located at the center of the gap between the signal and the ground lines. All experiments were performed at room temperature.

Figure 2(a) presents the in-plane (red) and out-of-plane (black) hysteresis loop of the YIG film measured by vibrating sample magnetometer (VSM). A clear easy axis loop is observed when the field has been swept along the in-plane direction. The sharp magnetic switching with tiny coercivity field (less than 0.1 mT) indicates the high quality of our YIG film with good magnetic uniformity and few pinning sites. The out-of-plane loop shows a typical hard-axis loop with the saturation field around ±150 mT. After capping with Ti/[Co/Pd]$_5$ multilayers, we observe a superposition of the linear background from the YIG film and a hysteretic behavior from [Co/Pd]$_5$ multilayers [black curve in Fig. 2(b)]. The magnetization flips at ±50 mT correspond to the magnetization reversal of the perpendicularly magnetized Co/Pd multilayers. Due to the strong PMA of the Co/Pd multilayers, the in-plane magnetic field within ±300 mT has negligible influence on the Co/Pd moments. Thus, the in-plane *M-H* loop only depicts the magnetization of YIG film even for YIG/Ti/[Co/Pd]$_5$. Further, the difference between the out-of-plane and in-plane hysteresis loops above ±150 mT in Fig. 2(b) represents the magnetic moments of Co/Pd multilayers. This is supported by the anomalous Hall effect (AHE) measurement of YIG/Ti/[Co/Pd]$_5$, which shows the same switching fields as the *M-H* loop [Fig. 2(b)]. Therefore, both the hysteresis loop and AHE measurements indicate that Ti/[Co/Pd]$_5$ possesses strong PMA, and with negligible coupling to the in-plane magnetized YIG film.

We next study the spin-charge conversion in Co/Pd multilayers with the spin pumping technique, in which the magnetization dynamics is excited by means of a broadband CPW. The Ti/$[Co/Pd]_5$ strip with 2 mm length and 20 $\mu$m width sits in the center of the 100-$\mu$m-wide gap between the signal line and ground line of the CPW (Fig. 3 inset). Microwave radiation from a variable-frequency microwave generator is used to power the CPW. In this geometry, the sample experiences mainly an out-of-plane rf magnetic field perpendicular to the external dc magnetic field, and the spin current contribution can be readily distinguished from other spurious signals [45]. The YIG film undergoes FMR when the external magnetic field and the microwave frequency satisfy the Kittel equation and meanwhile injects a spin current into the Ti/$[Co/Pd]_5$ multilayers, thus generating a charge current due to the ISHE or AISHE. In order to achieve high signal-to-noise level, a lock-in amplifier is used to modulate the applied microwave with the frequency of 17.9 kHz. Benefiting from the insulating YIG substrate, the spin rectification due to the anisotropic magnetoresistance (AMR), planar Hall effect (PHE), anomalous Hall effect and the precessing YIG's magnetization are largely diminished. Equally important, since the magnetizations of the Co/Pd multilayers and the YIG film are decoupled, it is not necessary to consider the spin rectification in the Co/Pd multilayers either. In addition, we have demonstrated recently that the spin pumping signal is free of thermoelectric contributions, including anomalous Nernst effect and spin Seebeck effect [46]. Therefore, the detected signal has pure spin pumping induced spin-charge conversion origin.

Before the spin pumping measurement, we first align the magnetization of the Co/Pd multilayers along the $+z$ direction with a strong magnetic field. Due to the strong PMA of Ti/$[Co/Pd]_5$, the magnetization orientation of the Co/Pd multilayers remains unchanged after withdrawing the out-of-plane field and while scanning the in-plane field. Figure 3(a) presents the spin pumping current in Ti/$[Co/Pd]_5$ with the sweeping magnetic field along the $y$ direction, where the microwave frequency is fixed at 9 GHz. In this geometry, the detected signal comes from ISHE in the Co/Pd multilayers. The spin pumping current exhibits a peak-and-dip pair appearing at $\pm$261 mT, with a symmetric Lorentzian line shape that corresponds to the FMR of the YIG layer, indicating its pure spin current origin. When the in-plane field sweep is applied along the $x$ direction, the ISHE induces a charge current flows along the $y$ direction, which is undetectable in our geometry. On the other hand, spin polarization along the $x$ direction can generate a charge current also along the $x$ direction through the AISHE. Figure 3(b) presents the measured spin pumping signal with the Co/Pd multilayers magnetized along the $+z$ direction when the in-plane field sweeps along the $x$ direction. Albeit with a reduced amplitude as compared to Fig. 3(a), the charge current peak/dip with symmetric Lorentzian line shape is also observed at the resonance fields of the YIG film. Consistent with the scenario of ISHE, we observe an identical spin pumping curve when $[Co/Pd]_5$ is aligned along the $-z$ direction [Fig. 3(c)]. More importantly, when the in-plane magnetic field sweeps along the $x$ direction and the magnetization of Co/Pd multilayers is aligned along the $-z$ direction [Fig. 3(d)], the curve reverses its polarity compared with Fig. 3(b), consistent with the prediction of AISHE in the ferromagnet as discussed above [18]. Thus, we have unambiguously observed the spin-charge conversion via the AISHE. And the direction of the converted current via the AISHE of Co/Pd is aligned the direction of $\hat{j}_s \times (\hat{M}_{\mathrm{Co/Pd}} \times \hat{M}_{\mathrm{YIG}})$. This result is in good agreement with previous studies obtained by spin torque measurements in Pt/Co bilayer [29,31], thermoelectric measurement in Pt/Co/Pt trilayer [34], and $Tb_xCo_{100-x}$ alloy with the magnetization dominated by Co [35]. The weak asymmetry of the amplitude of the AISHE measured at positive/negative fields is due to the non-negligible contribution of the rf magnetic field along the $y$ direction [47]. When we performed the measurement with the sample strip placed at the other side of the CPW, the symmetry was reversed (not shown). For comparison, we also measured the spin pumping signal of Ti(3 nm)/Pd(12.2 nm) at 9 GHz with sweeping field along the $y$ direction [Fig. 3(e)] and along the $x$ direction [Fig. 3(f)], respectively. We find that the sign of ISHE of the Co/Pd multilayers is the same as that of Pd. It should be noted that there is no spin pumping signal when the magnetic field is applied along the $x$ direction for Ti/Pd.

We next discuss the influence of the possible artifacts from the slight field misalignment and the spin rectification effect. To exclude the potential artifacts caused by the field misalignment, we performed the angular dependent

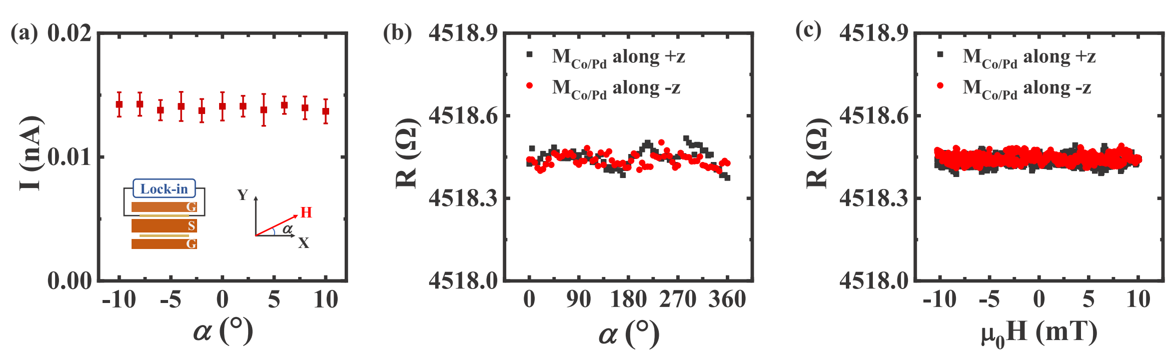


FIG. 4. (a) The spin pumping signal difference between the magnetization of Co/Pd multilayers along $+z$ and $-z$ at 9 GHz within 10° of the $x$ direction in the $xy$ plane. The signal is the average of that in $+H$ and $-H$. The resistance of YIG/Ti/$[Co/Pd]_5$ strip as a function of (b) in-plane angle with a constant external magnetic field 20 mT, and (c) magnetic field along $y$ direction, respectively. The black square and red circle represent the resistance when the magnetization of Co/Pd multilayers is along $+z$ and $-z$, respectively.

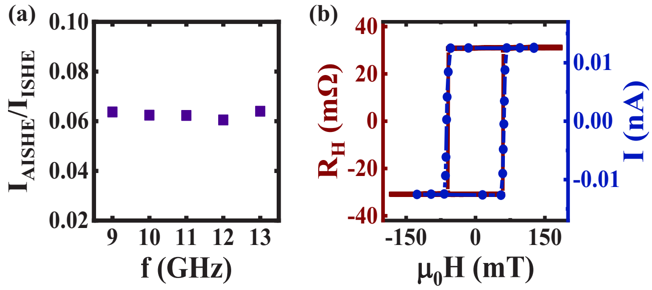


FIG. 5. (a) The frequency dependent ratio of the amplitudes of AISHE signal to ISHE signal. (b) Comparison of the hysteresis loops measured by AHE (brown) and AISHE (blue) for Co/Pd multilayers.

measurements by varying the angle between the external field and the $x$ direction within 10° in the $xy$ plane. As shown in Fig. 4(a), the measured AISHE (the half value of the difference obtained with the magnetization of Co/Pd multilayers along $+z$ and $-z$) shows little angular dependence within our experimental error margin. This confirms that the detected AISHE in Co/Pd multilayers is not due to the possible slight field misalignment. It is further supported by the fact that there is no apparent AISHE signal in the YIG/Ti/Pd system, as presented in Fig. 3(f). In addition, we also performed the angular dependent [Fig. 4(b)] and field dependent [Fig. 4(c)] magnetoresistance measurements of YIG/Ti/$[Co/Pd]_5$; both yield negligible spin Hall magnetoresistance (SMR) within our experimental error margin (below 0.002%), and the AHE and PHE exhibit a similar order of magnitude for the ferromagnetic insulator/normal metal bilayers [48,49]. Thus, we believe that the spin rectifications due to SMR (AMR), PHE, and AHE are negligible. In addition, we did not observe any apparent antisymmetric Lorentzian shape line in our results at different frequencies, corroborating negligible spin rectifications.

The conventional ISHE induced current $I_{ISHE}$ in $[Co/Pd]_5$ is around 0.22 nA [Figs. 3(a) and 3(c)], while the anomalous ISHE induced current $I_{AISHE}$ is around 0.014 nA [Figs. 3(b) and 3(d)]. The ratio of $I_{AISHE}/I_{ISHE}$ is roughly a constant (6.3%) when the microwave frequency varies between 9 and 13 GHz [Fig. 5(a)], indicating it is a material specific parameter, and the $I_{AISHE}/I_{ISHE}$ ratio in $[Co/Pd]_5$ we find herein is higher than that of Pt/Co/Pt [34] but lower than $Tb_xCo_{100-x}$ [35], indicating AISHE can be easily regulated. Our results also cast further investigations of ASHE and AISHE by engineering the ferromagnet materials.

Last, we establish the direct correlation between the AISHE and the out-of-plane magnetization of the $[Co/Pd]_5$ multilayers. We begin with the saturation of the $[Co/Pd]_5$ with a +200-mT perpendicular magnetic field $H_z$. This field is gradually ramped down to a certain negative reversal field $H_R$ and then back to zero. After that, we perform the AISHE measurement with sweeping in-plane $H_x$. The above-mentioned procedures are performed repeatedly until $H_R$ is lower than the negative coercivity field of $[Co/Pd]_5$ multilayers. The same experiments are also performed for positive $H_R$ starting from saturation of the $[Co/Pd]_5$ with a −200-mT field along the $z$ direction. The $H_R$ dependent $I_{AISHE}$ is then plotted as blue dots in Fig. 5(b). Remarkably, we find the AISHE loop coincides with the AHE signal of a Hall bar strip with the same width. Our results show that the AISHE in the ferromagnet is linearly correlated with its magnetization, consistent with the prediction based on the general tensor requirement of the anomalous inverse spin Hall angle [Eq. (2)]. Thus, we observed all the three distinguished features of AISHE in comparison with ISHE and established the solid evidence for the AISHE.

In summary, we have performed the spin-charge conversion studies of the perpendicularly magnetized $[Co/Pd]_5$ multilayers with spin pumping measurements. Both the conventional ISHE with charge current orthogonal to the spin polarization and the anomalous ISHE with charge current parallel with the spin polarization are observed, with a fixed ratio independent of the applied microwave frequency. Furthermore, we also reported the linear relation between the AISHE and out-of-plane magnetization of $[Co/Pd]_5$ multilayers. ASHE and AISHE in the ferromagnet enrich the spin transport studies, wherein the symmetry breaking due to order parameters magnetization **M** may pave a way for searching for novel spintronics materials.

This work was supported by the National Key R&D Program of China (Grants No. 2018YFA0306004 and No. 2017YFA0303202), the National Natural Science Foundation of China (Grants No. 11974165, No. 11974296, No. 51971110, No. 92165103, No. 11734006, and No. 11727808), and the Natural Science Foundation of Jiangsu Province (Grant No. BK20190057). X.R.W. was supported by Hong Kong RGC (Grants No. 16301518, No. 16301619, and No. 16302321).

[1] J. Sinova, S. O. Valenzuela, J. Wunderlich, C. H. Back, and T. Jungwirth, Rev. Mod. Phys. **87**, 1213 (2015).
[2] A. Hirohata, K. Yamada, Y. Nakatani, I. L. Prejbeanu, B. Dieny, P. Pirro, and B. Hillebrands, J. Magn. Magn. Mater. **509**, 166711 (2020).
[3] L. Q. Liu, O. J. Lee, T. J. Gudmundsen, D. C. Ralph, and R. A. Buhrman, Phys. Rev. Lett. **109**, 096602 (2012).
[4] L. Q. Liu, C. F. Pai, Y. Li, H. W. Tseng, D. C. Ralph, and R. A. Buhrman, Science **336**, 555 (2012).
[5] I. M. Miron, K. Garello, G. Gaudin, P. J. Zermatten, M. V. Costache, S. Auffret, S. Bandiera, B. Rodmacq, A. Schuhl, and P. Gambardella, Nature (London) **476**, 189 (2011).
[6] L. Caretta, S. H. Oh, T. Fakhrul, D. K. Lee, B. H. Lee, S. K. Kim, C. A. Ross, K. J. Lee, and G. S. D. Beach, Science **370**, 1438 (2020).
[7] W. J. Jiang, P. Upadhyaya, W. Zhang, G. Q. Yu, M. B. Jungfleisch, F. Y. Fradin, J. E. Pearson, Y. Tserkovnyak, K. L. Wang, O. Heinonen *et al.*, Science **349**, 283 (2015).
[8] F. Oboril, R. Bishnoi, M. Ebrahimi, and M. B. Tahoori, IEEE Trans. Comput. Aided Des. Integr. Circuits Syst. **34**, 367 (2015).
[9] Y. Zhang, H. Y. Yuan, X. S. Wang, and X. R. Wang, Phys. Rev. B **97**, 144416 (2018).

[10] R. Li, S. Zhang, S. Luo, Z. Guo, Y. Xu, J. Ouyang, M. Song, Q. Zou, L. Xi, X. Yang *et al.*, Nat. Electron. **4**, 179 (2021).
[11] Z. Luo, A. Hrabec, T. P. Dao, G. Sala, S. Finizio, J. Feng, S. Mayr, J. Raabe, P. Gambardella, and L. J. Heyderman, Nature (London) **579**, 214 (2020).
[12] C. F. Pai, L. Q. Liu, Y. Li, H. W. Tseng, D. C. Ralph, and R. A. Buhrman, Appl. Phys. Lett. **101**, 122404 (2012).
[13] D. MacNeill, G. M. Stiehl, M. H. D. Guimaraes, R. A. Buhrman, J. Park, and D. C. Ralph, Nat. Phys. **13**, 300 (2017).
[14] G. Yu, P. Upadhyaya, Y. Fan, J. G. Alzate, W. Jiang, K. L. Wong, S. Takei, S. A. Bender, L. T. Chang, Y. Jiang *et al.*, Nat. Nanotechnol. **9**, 548 (2014).
[15] Y. W. Oh, S. H. Chris Baek, Y. M. Kim, H. Y. Lee, K. D. Lee, C. G. Yang, E. S. Park, K. S. Lee, K. W. Kim, G. Go *et al.*, Nat. Nanotechnol. **11**, 878 (2016).
[16] A. van den Brink, G. Vermijs, A. Solignac, J. Koo, J. T. Kohlhepp, H. J. M. Swagten, and B. Koopmans, Nat. Commun. **7**, 10854 (2016).
[17] Q. Ma, Y. Li, D. B. Gopman, Y. P. Kabanov, R. D. Shull, and C. L. Chien, Phys. Rev. Lett. **120**, 117703 (2018).
[18] X. R. Wang, Commun. Phys. **4**, 55 (2021).
[19] M. Kimata, H. Chen, K. Kondou, S. Sugimoto, P. K. Muduli, M. Ikhlas, Y. Omori, T. Tomita, A. H. MacDonald, S. Nakatsuji *et al.*, Nature (London) **565**, 627 (2019).
[20] Y. Liu, Y. Liu, M. Chen, S. Srivastava, P. He, K. L. Teo, T. Phung, S.-H. Yang, and H. Yang, Phys. Rev. Appl. **12**, 064046 (2019).
[21] X. Chen, S. Shi, G. Shi, X. Fan, C. Song, X. Zhou, H. Bai, L. Liao, Y. Zhou, H. Zhang *et al.*, Nat. Mater. **20**, 800 (2021).
[22] M. H. D. Guimaraes, G. M. Stiehl, D. MacNeill, N. D. Reynolds, and D. C. Ralph, Nano Lett. **18**, 1311 (2018).
[23] L. Liu, C. Zhou, X. Shu, C. Li, T. Zhao, W. Lin, J. Deng, Q. Xie, S. Chen, J. Zhou *et al.*, Nat. Nanotechnol. **16**, 277 (2021).
[24] M. B. Lifshits and M. I. Dyakonov, Phys. Rev. Lett. **103**, 186601 (2009).
[25] V. P. Amin, J. Zemen, and M. D. Stiles, Phys. Rev. Lett. **121**, 136805 (2018).
[26] S. C. Baek, V. P. Amin, Y. W. Oh, G. Go, S. J. Lee, G. H. Lee, K. J. Kim, M. D. Stiles, B. G. Park, and K. J. Lee, Nat. Mater. **17**, 509 (2018).
[27] C. O. Pauyac, M. Chshiev, A. Manchon, and S. A. Nikolaev, Phys. Rev. Lett. **120**, 176802 (2018).
[28] A. M. Humphries, T. Wang, E. R. J. Edwards, S. R. Allen, J. M. Shaw, H. T. Nembach, J. Q. Xiao, T. J. Silva, and X. Fan, Nat. Commun. **8**, 911 (2017).
[29] T. Wang, S. Lendinez, M. B. Jungfleisch, J. Kolodzey, J. Q. Xiao, and X. Fan, Appl. Phys. Lett. **116**, 012404 (2020).
[30] Y. Hibino, K. Hasegawa, T. Koyama, and D. Chiba, APL Mater. **8**, 041110 (2020).
[31] Y. Hibino, T. Moriyama, K. Hasegawa, T. Koyama, T. Ono, and D. Chiba, Appl. Phys. Express **13**, 083001 (2020).
[32] Y. Hibino, K. Yakushiji, A. Fukushima, H. Kubota, and S. Yuasa, Phys. Rev. B **101**, 174441 (2020).
[33] Y. Hibino, T. Taniguchi, K. Yakushiji, A. Fukushima, H. Kubota, and S. Yuasa, Nat. Commun. **12**, 6254 (2021).
[34] T. C. Chuang, D. Qu, S. Y. Huang, and S. F. Lee, Phys. Rev. Research **2**, 032053(R) (2020).
[35] A. Yagmur, S. Sumi, H. Awano, and K. Tanabe, Phys. Rev. B **103**, 214408 (2021).
[36] S. Iihama, T. Taniguchi, K. Yakushiji, A. Fukushima, Y. Shiota, S. Tsunegi, R. Hiramatsu, S. Yuasa, Y. Suzuki, and H. Kubota, Nat. Electron. **1**, 120 (2018).
[37] Y. Tserkovnyak, A. Brataas, and G. E. W. Bauer, Phys. Rev. Lett. **88**, 117601 (2002).
[38] Y. Tserkovnyak, A. Brataas, and G. E. W. Bauer, Phys. Rev. B **66**, 224403 (2002).
[39] E. Saitoh, M. Ueda, H. Miyajima, and G. Tatara, Appl. Phys. Lett. **88**, 182509 (2006).
[40] J. J. Ding, T. Liu, H. C. Chang, and M. Z. Wu, IEEE Magn. Lett. **11**, 5502305 (2020).
[41] A. V. Davydenko, A. G. Kozlov, A. V. Ognev, M. E. Stebliy, A. S. Samardak, K. S. Ermakov, A. G. Kolesnikov, and L. A. Chebotkevich, Phys. Rev. B **95**, 064430 (2017).
[42] X. D. Tao, Q. Liu, B. F. Miao, R. Yu, Z. Feng, L. Sun, B. You, J. Du, K. Chen, S. F. Zhang *et al.*, Sci. Adv. **4**, eaat1670 (2018).
[43] B. F. Miao, S. Y. Huang, D. Qu, and C. L. Chien, Phys. Rev. Lett. **111**, 066602 (2013).
[44] D. Tian, Y. Li, D. Qu, S. Y. Huang, X. Jin, and C. L. Chien, Phys. Rev. B **94**, 020403(R) (2016).
[45] K. He, J. Cheng, M. Yang, Y. H. Zhang, L. Q. Yu, Q. Liu, L. Sun, B. F. Miao, C. M. Hu, and H. F. Ding, Phys. Rev. B **105**, 104406 (2022).
[46] J. Cheng, K. He, M. Yang, Q. Liu, R. Yu, L. Sun, J. J. Ding, B. F. Miao, M. Z. Wu, and H. F. Ding, Phys. Rev. B **103**, 014415 (2021).
[47] L. Bai, Z. Feng, P. Hyde, H. F. Ding, and C. M. Hu, Appl. Phys. Lett. **102**, 242402 (2013).
[48] Q. Shao, C. Tang, G. Yu, A. Navabi, H. Wu, C. He, J. Li, P. Upadhyaya, P. Zhang, S. A. Razavi *et al.*, Nat. Commun. **9**, 3612 (2018).
[49] C. O. Avci, A. Quindeau, C.-F. Pai, M. Mann, L. Caretta, A. S. Tang, M. C. Onbasli, C. A. Ross, and G. S. D. Beach, Nat. Mater. **16**, 309 (2017).